JACS
JOURNAL OF THE AMERICAN CHEMICAL SOCIETY
Article
pubs.acs.org/JACS

Dangerous Liaisons between Detergents and Membrane Proteins. The Case of Mitochondrial Uncoupling Protein 2

Manuela Zoonens,[†,‡] Jeffrey Comer,[§,⊥] Sandrine Masscheleyn,[†,‡] Eva Pebay-Peyroula,[∥,#,⊗] Christophe Chipot,[§,⊥,▽] Bruno Miroux,*[,†,‡] and François Dehez*[,§,⊥,▽]

[†]CNRS UMR 7099, Institut de Biologie Physico Chimique (IBPC), 75005 Paris, France
[‡]Université Paris-Diderot, IBPC, 75005 Paris, France
[§]CNRS UMR 7565, Structure et Réactivité des Systèmes Moléculaires Complexes (SRSMC), 54500 Vandoeuvre-les-Nancy, France
[⊥]Université de Lorraine, SRSMC, 54500 Vandoeuvre-les-Nancy, France
[∥]Université Grenoble Alpes, Institut de Biologie Structurale (IBS), F-38027 Grenoble, France
[#]CEA, DSV, IBS, F-38027 Grenoble, France
[⊗]CNRS, IBS, F-38027 Grenoble, France
[▽]Laboratoire International Associé CNRS and University of Illinois at Urbana−Champaign, 54506 Vandoeuvre-lès-Nancy, France

Supporting Information

ABSTRACT: The extraction of membrane proteins from their native environment by detergents is central to their biophysical characterization. Recent studies have emphasized that detergents may perturb the structure locally and modify the dynamics of membrane proteins. However, it remains challenging to determine whether these perturbations are negligible or could be responsible for misfolded conformations, altering the protein's function. In this work, we propose an original strategy combining functional studies and molecular simulations to address the physiological relevance of membrane protein structures obtained in the presence of detergents. We apply our strategy to a structure of isoform 2 of an uncoupling protein (UCP2) binding an inhibitor recently obtained in dodecylphosphocholine detergent micelles. Although this structure shares common traits with the ADP/ATP carrier, a member of the same protein family, its functional and biological significance remains to be addressed. In the present investigation, we demonstrate how dodecylphosphocholine severely alters the structure as well as the function of UCPs. The proposed original strategy opens new vistas for probing the physiological relevance of three-dimensional structures of membrane proteins obtained in non-native environments.

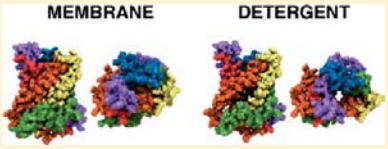

INTRODUCTION

Uncoupling proteins (UCPs) belong to the mitochondrial anion carrier family (MCF) (for reviews, see Rousset et al.[1] and Kunji[2]). Uncoupling protein 1 (UCP1) is exclusively found in mitochondria of brown adipocytes of mammals, where it increases the inner mitochondrial membrane permeability to protons. As a consequence, the energy from substrate oxidation stored in the electrochemical proton gradient does not promote ATP synthesis, but is dissipated. Both in vivo[3] and in vitro experiments[4−7] reflect the proton transport activity of UCP1 activated by free fatty acids and inhibited by purine nucleotides.[8] The mechanism of proton transport is, however, controversial. Several MCFs are able to perform free-fatty-acid cycling through the inner mitochondrial membrane by facilitating the pathway of fatty acids in their charged form from the internal to the external leaflet of the membrane (see Table 2 in Rial et al.[9]). Yet, the physiological relevance of this mechanism is still contentious, not only for UCP1, but also for UCP2 and UCP3, which are clearly not physiological uncouplers.[10,11] Patch-clamp measurements on isolated brown fat mitochondria have recently revealed that UCP1 is a fatty acid/proton symporter with an aborted transport for long-chain fatty acids.[12] This evidence is strongly in favor of a second model for UCP transport mechanism, in which fatty acids play a catalytic function.[13,14] In contrast to UCP1, the physiological function of UCP2 is linked with reactive oxygen species regulation in immune cells and neurons.[15−17] At the cellular level, UCP2 promotes fatty acid oxidation without detectable uncoupling of respiration, and its metabolite transport activity is still a matter of debate (for review, see Bouillaud[18]).

However challenging, structural investigation of the MCF is crucial for the understanding of transport mechanisms and regulation. Several strategies have been developed to overcome the low natural abundance of most of the carriers. Kunji and collaborators succeeded in producing the ADP/ATP carrier (AAC) from yeast mitochondria and in obtaining a two-dimensional projection map of the carrier.[20] A high-resolution structure of bovine AAC was obtained by three-dimensional crystallization of the protein isolated from natural sources.[21] The presence of a conserved motif repeated three times along the sequence between members of the MCF suggest a common

Received: July 19, 2013
Published: September 10, 2013

dx.doi.org/10.1021/ja407424v | J. Am. Chem. Soc. 2013, 135, 15174−15182

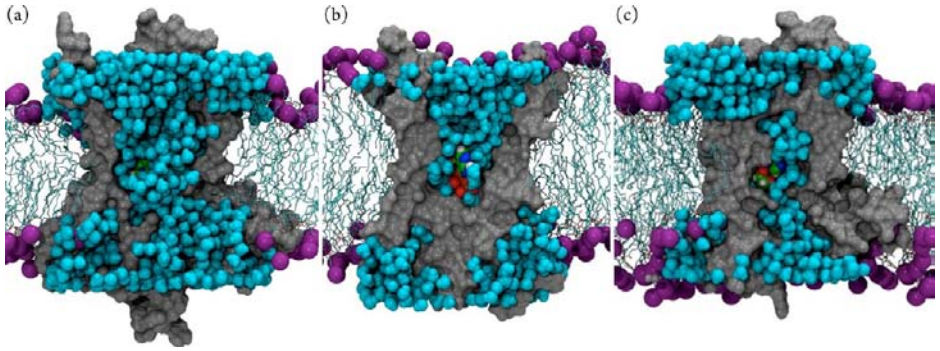

Figure 1. The UCP2 NMR structure acts as a large transmembrane channel. (a) Cross-sectional view of UCP2-GDP embedded in a POPC bilayer. Backbone atoms are constrained to their original positions in pdb:2LCK. A large water channel spanning the entire protein connects the two sides of the membrane. (b) Cross-sectional view of AAC-ADP^{3-} embedded in a POPC bilayer.[19] The protein is fully occluded on the matrix side and prevents water from crossing the bilayer. (c) Cross-sectional view of UCP2-GDP^{3-} embedded in a POPC bilayer after full relaxation of the entire protein. The large water channel observed in the backbone-constrained simulation collapses rapidly, leading to a markedly reduced internal cavity, occluded toward the intermembrane space. The protein surface is colored in gray. Violet and cyan spheres represent phospholipid headgroups and water molecules, respectively. Phosphorus, nitrogen, oxygen, and carbon atoms of GDP^{3-} and ADP^{3-} are colored in brown, blue, red, and green, respectively.

three-dimensional fold. This assumption was strengthened by the low-resolution structure of UCP2 obtained recently by a cutting-edge strategy based on solution-state NMR and molecular fragment replacement.[22] Even armed with such an advanced methodology, solving membrane protein structures remains challenging, and requires detergent to extract these biological macromolecules from their native environments. How different the structure of the membrane protein in detergents is from its membrane-bound state remains difficult to predict. Previous studies suggest that the replacement of natural lipids by detergents could modify to different extents the structure and/or the dynamics of membrane proteins.[23−30] The question of whether or not the detergents may favor non-native conformations, which in turn would alter the protein function, has remained hitherto elusive.

The comparison of the UCP2 structure with that of AAC indeed gives rise to some concerns related to structural differences possibly due to the surrounding detergent. The structures of AAC and UCP2 were solved in the presence of zwitterionic detergents, LAPAO and DPC respectively, and in the presence of inhibitors, namely carboxyatractyloside for AAC and GDP^{3-} for UCP2. Yet, if the structure of AAC is admittedly very compact, that of UCP2 appears looser and features unusual cavities between transmembrane spans with polar residues exposed at the surface of the hydrophobic region of the protein. Furthermore, the relative organization of glycine residues obliterates their participation in the helix packing, in stark contrast with AAC.[31] Given the unexpected NMR model of UCP2, we endeavored to investigate the conformational stability of UCP2 both in detergent and in a lipid bilayer by means of molecular dynamics (MD) simulations. The MD approach is particularly suited to unveil the dynamics of chemical and biological systems at the atomistic level. It is widely used to investigate the behavior of membrane proteins in a lipid environment and, hence, can complement structural data obtained in detergent solution. MD was recently employed to study the mitochondrial AAC, confirming that the structure solved in the presence of a specific inhibitor is also capable of binding spontaneously its endogenous nucleotide substrates.[19,32,33] Here, we show that UCP2 behaves as a pore in DPC, but rapidly collapses in a lipid environment, suggesting that the structure of UCP2 in DPC does not reflect the membrane-bound, functional conformation. To rationalize this finding, we tested the effect of DPC on UCP1 and UCP2 activities after purification from native and recombinant sources, respectively. Our results indicate that DPC is not a suitable detergent to maintain the activity of either UCP1 or UCP2, and suggest that it should be avoided in structural studies of mitochondrial uncoupling proteins.

RESULTS

Molecular Dynamics Simulation of UCP2 with Its Backbone Constrained to the NMR Structure in a Membrane-like Environment. The NMR structure of UCP2[22] (successively with and without GDP^{3-}) was embedded in a bilayer of pure 1-palmitoyl-2-oleoyl-*sn*-glycero-3-phosphatidyl-choline (POPC). After proper equilibration of the lipids, water and GDP^{3-}, the side chains were progressively allowed to relax for 10 ns while the backbone atoms were kept fixed to their NMR positions (see Methods). The dynamics of water and the topology of the internal cavity of the protein were analyzed in the subsequent 10 ns (Figure 1a). The results were compared to the data accrued previously for AAC in the same environment[19] (Figure 1b). In its NMR structure, UCP2 mainly consists of a large water channel that spans the entire protein and connects both sides of the membrane, irrespective of the presence of GDP^{3-} (see Supporting Information, Figure S1). In the narrowest region of the protein, the effective radius of the internal cavity of the spatially constrained UCP2 is about 6.1 Å, at variance with AAC, which is fully occluded over approximately 10 Å on the matrix side[19,34] (see Figure 2). This large cavity radius resembles the size of constriction regions in pore-forming proteins, e.g., α-hemolysin,[35] and in bacterial outer-membrane proteins,[36] which convey in a nonselective fashion a variety of substrates across the membrane. To reinforce this analysis and exclude a putative intermediary transport state of UCP2, the osmotic permeability (P_f) for water of the constrained UCP2 was estimated following the method of Zhu et al.[37] For constrained UCP2 in the absence of GDP^{3-}, $P_f = (0.53 \pm 0.02) \times 10^{-12}$ cm^3/s, while it is $(0.32 \pm 0.02) \times 10^{-12}$ cm^3/s for constrained UCP2 binding GDP^{3-}. This value is only 4 times smaller than the corresponding quantity calculated for α-hemolysin, 1.9×10^{-12} cm^3/s.[35] The qualitative behavior of UCP2 NMR structure is, therefore,

dx.doi.org/10.1021/ja407424v | J. Am. Chem. Soc. 2013, 135, 15174−15182

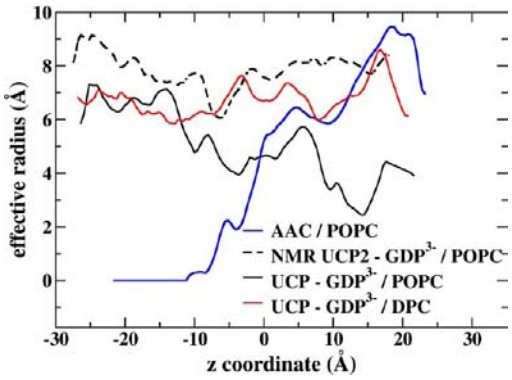

Figure 2. Effective radii of UCP2 and AAC internal cavities for (i) UCP2 binding GDP^{3-} embedded in POPC with the backbone frozen in its NMR conformation by means of holonomic constraints (dashed black line), (ii) UCP2 binding GDP^{3-} embedded in POPC with the backbone fully relaxed (black line), (iii) UCP2 binding GDP^{3-} embedded in DPC with the backbone fully relaxed (red line), and (iv) AAC embedded in POPC with the backbone fully relaxed (blue line), plotted as a function of the distance from the center of mass of the protein along the z axis.

closer to that of a porin than that of an occluded transmembrane protein like AAC, for which P_f is formally zero.

Molecular Dynamics Simulation of UCP2 Fully Relaxed in a Membrane-like Environment. For UCP2 associated to GDP^{3-}, the MD trajectory was extended further up to 175 ns without any positional holonomic constraint (a function that depends only on the atomic coordinates and the time, Figure 1c).

In sharp contrast with the majority of membrane proteins studied by MD, UCP2 quickly moves away from its initial reference structure as reflected in a large root-mean-square-deviation (RMSD) of the backbone atoms of about 6 Å (see Figure S2). Moreover, the decrease of both the radius of gyration (R_g) and the solvent-accessible surface area (SASA) measured in pdb:2LCK from 22.9 Å and 22 900 $Å^2$ to mean values of 20.9 Å and 16 300 $Å^2$, respectively, is representative of a collapse of UCP2 toward a more compact structure (see Figure 3b,c). This alteration is illustrated further by a pronounced decrease of the effective radius of the internal cavity (see Figure 2). The overall volume of the cavity is reduced by 60%, and, in its narrowest region, the effective radius is 2.4 Å. Although the fully relaxed structure appears much more occluded than the NMR reference, the water osmotic permeability still remains appreciable, $P_f = (0.11 \pm 0.01) \times 10^{-12}$ cm^3/s, suggesting that the collapsed structure is unlikely to correspond to the actual membrane-bound structure.

The UCP2 NMR structure is organized in a bundle of six integral helices, but unlike AAC,[21] packing of this bundle appears suboptimal, presenting numerous cavities between transmembrane spans (see Figure 3a). Their surface exposes not only hydrophobic residues to the core of the bilayer but also many polar amino acids (see Figure S3). In the constrained-backbone simulation, lipid tails fill interhelix cavities. When the constraints are eliminated, lipids rapidly move away from these interstices, allowing the helices to couple tightly, which in turn lowers the exposure of polar residues toward the membrane hydrophobic core and is responsible for the collapse of the initial NMR structure. It should be emphasized that brute-force MD simulations, due to current computational limitations, cannot capture slow processes like folding of large proteins. Our data, therefore, only highlight that the UCP2 NMR structure is not stable in a lipid bilayer environment (see Figure 1c and Figure S4). In the following section, we test the conclusions from the MD simulations by measuring the activities of UCP1 and UCP2 in liposomes after purification in DPC.

Loss of Activities of UCP1 and UCP2 after Being Purified in DPC. There is no abundant natural source of UCP2. Therefore native UCP1 was selected as a reference of native mitochondrial uncoupling protein. UCP1 is closely related to UCP2 with 57% of sequence identity. The effect of DPC was compared with that of Triton X-100, a relatively mild detergent known to preserve the activity of mitochondrial carriers.[38,39] Native UCP1 from brown adipose tissue (BAT) of mice was solubilized and purified in Triton X-100 and in DPC while recombinant UCP2 overexpressed in *E. coli* was solubilized from a pellet containing bacterial membranes and cell fragments and then purified in DPC (see Figure 4a). The proton-transport activity of UCP1 was measured after reconstitution in liposomes loaded with KCl. The ΔpH formed after addition of nigericin was converted into ΔΨ when proton transport occurred through UCP1 (see Figure 4b). The electric potential was measured by recording the absorbance at 520 nm of the safranine O, which aggregates as a function of the membrane potential.[6] When purified in Triton X-100, proton-transport activity of UCP1 was strongly enhanced by the presence of 30 μM lauric acid and fully inhibited by addition of 50 μM GDP^{3-} (see Figure 5). In contrast, when UCP1 was purified in DPC, lauric acid had no significant activating effect on proton transport, and, as a consequence, no eventual inhibitory effect of GDP^{3-} could be measured. Next, the free-fatty-acid-dependent protonophoric activity of UCP2 was investigated. No proton-transport activity was observed when the protein was purified in DPC. Altogether, our results suggest that exposure to DPC severely compromises the proton-transport activity of both UCP1 and UCP2. In order to explain the irreversible inactivating effect of DPC, MD simulations in this detergent were performed on the structure of UCP2 obtained by NMR.

Molecular Dynamics Simulation of UCP2 Fully Relaxed in DPC. The interaction of DPC with the NMR structure of UCP2 was investigated by means of MD simulations. Bond et al.[25,40] have shown that DPC aggregation time around membrane proteins is short enough to be described by MD. Using all-atom and coarse-grained simulations, they were able to reproduce the self-assembly of detergents into a ring-shape bundle around the hydrophobic core of gramicidin A and OmpF, a common feature observed with membrane proteins.[41,42] All-atom and coarse-grained MD simulations were carried out starting from randomly disperse solutions of DPC surrounding a single UCP2 protein constrained to its NMR structure (see Supplementary Methods). Qualitatively, the ring-shape bundle of DPC systematically forms around UCP2 on a time scale consistent with previous studies.[25,40] Interestingly enough, protein amphiphilic segments exposed to the solvent on the cytoplasmic (residues 298−308) and the matrix (residues 29−59) sides catalyze the formation of two additional detergent micelles (see Figure S5).

Based on the information yielded by the MD simulations, an initial model was built, in which all monitored DPC-protein interactions were, whenever possible, integrated. It consists of a

dx.doi.org/10.1021/ja407424v | J. Am. Chem. Soc. 2013, 135, 15174−15182

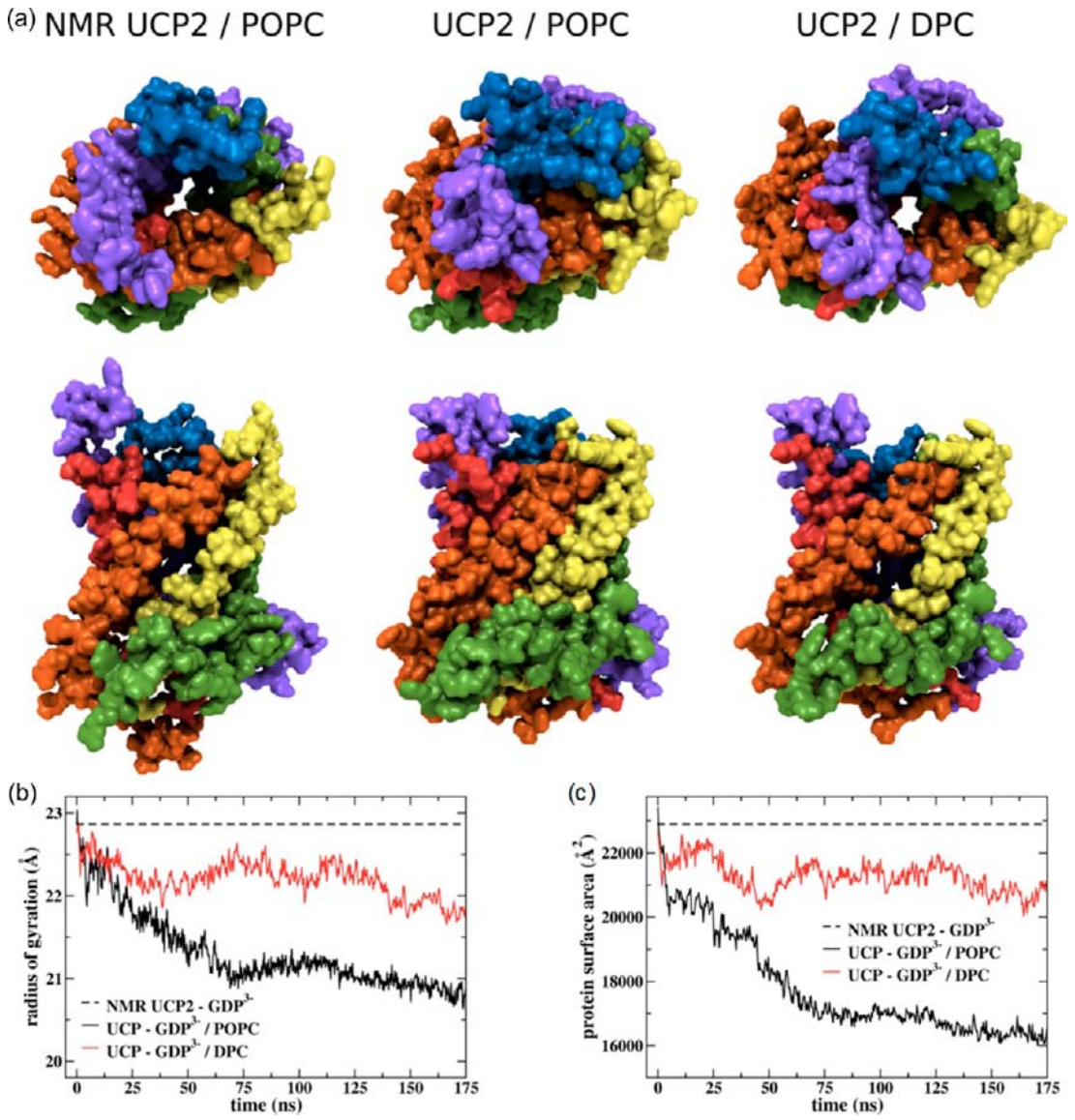

Figure 3. (a) Top and side views of three UCP2-GDP^{3-} complexes from simulations beginning with the pdb:2LCK structure. (Left) UCP2-GDP^{3-} in a POPC bilayer after 26 ns with its backbone holonomically constrained to the PDB structure. (Middle) UCP2-GDP^{3-} in a POPC bilayer after 175 ns, bereft of holonomic constraints or harmonic restraints. (Right) UCP2-GDP in the presence of 300 DPC detergent molecules after 175 ns, bereft of holonomic constraints or harmonic restraints. The top and bottom images show UCP2 from above the bilayer and in the plane of the bilayer, respectively. The protein DPC is aligned consistently with the views obtained for the constrained complex. For clarity, ions and water molecules, lipids, and detergents are not shown. (b) Radius of gyration of the UCP2 backbone atoms as a function of time for each one of the three systems. The constant value for the system where the backbone is constrained to that of the PDB structure is shown as a dashed black horizontal line. (c) Surface area of the protein as a function of time for each one of the three systems. The constant value for the system where the backbone is constrained to that of the PDB structure is shown as a dashed black horizontal line. In (a), each helix is colored differently.

200-μM solution of detergent, composed of 300 DPC molecules lying on the surface and in the internal cavity of UCP2. After proper equilibration of DPC around the constrained protein, the entire system was fully relaxed for 175 ns. The RMSD of backbone-atom positions converges toward a value of about 4.5 Å, corresponding to a lesser degree of reorganization than observed in the POPC simulation (see Figure S2). The topology of the overall NMR UCP2 structure is retained, as suggested by the effective radius of the internal cavity, in line with the NMR conformation (see Figure 2). Similarly, the water osmotic permeability, $(0.32 \pm 0.01) \times 10^{-12}$ cm^3/s, agrees nicely with the value calculated for UCP2 with backbone atoms constrained to their NMR positions. The evolution of R_g and SASA further confirms that in MD simulations in DPC, UCP2 retains a structure akin to the NMR one (see Figure 3). Interstitial spaces between helices are stabilized not only by the hydrophobic tails of DPC, but also by its polar head groups. The amphiphilic segments lying on both sides of the protein are steadily encapsulated into micelles of a size compatible with their solution counterpart[43] (see Figure 6). The small length of the DPC chain combined with its flexibility allows for precise targeting of every amphiphilic patches lying all over the exposed surface of the protein. About three DPC molecules are trapped at the edges of the internal cavity, in regions wide enough to not significantly affect the water osmotic permeability. Continuity of the ring-shape bundle of detergents around the protein is interrupted (see Figure 6). This disruption stems from a groove of polar

dx.doi.org/10.1021/ja407424v | J. Am. Chem. Soc. 2013, 135, 15174−15182

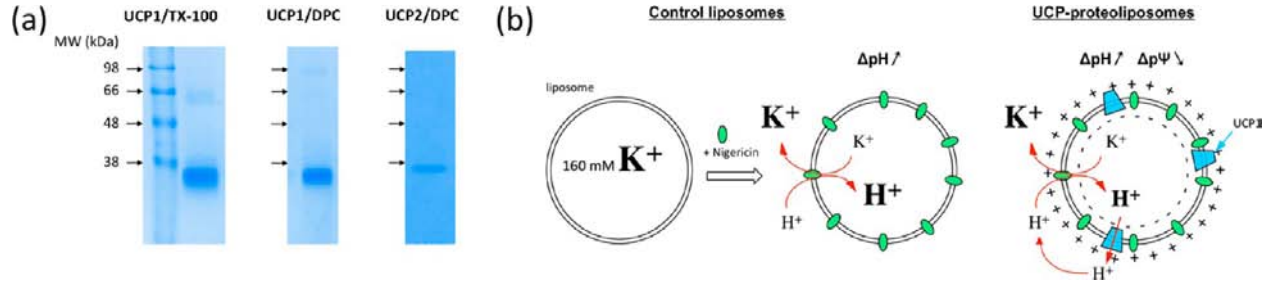

Figure 4. UCP1 and UCP2 samples after purification. (a) SDS-PAGE of UCP1 purified from mitochondria of brown adipocytes of mice in either Triton X-100 or DPC and mouse UCP2 overexpressed in *E. coli* and purified in DPC (see the Methods section). (b) Schematic representation of the liposomes assay setup. Liposomes are loaded with 160 mM potassium ions. The antibiotic nigericin is a potassium/proton ionophore. In the absence of UCP (control), a ΔpH is generated by exchanging potassium ions against protons. However, no signal is detected because the colorimetric probe (safranine O) present in solution is not pH-sensitive. In the presence of UCP1 (sample), the protons accumulated inside the vesicles are transported outside following the protons gradient created by nigericin. The ΔpH is converted into a ΔΨ, which is detected by the membrane potential-sensitive probe safranine O (for further details see Mozo et al.[6]).

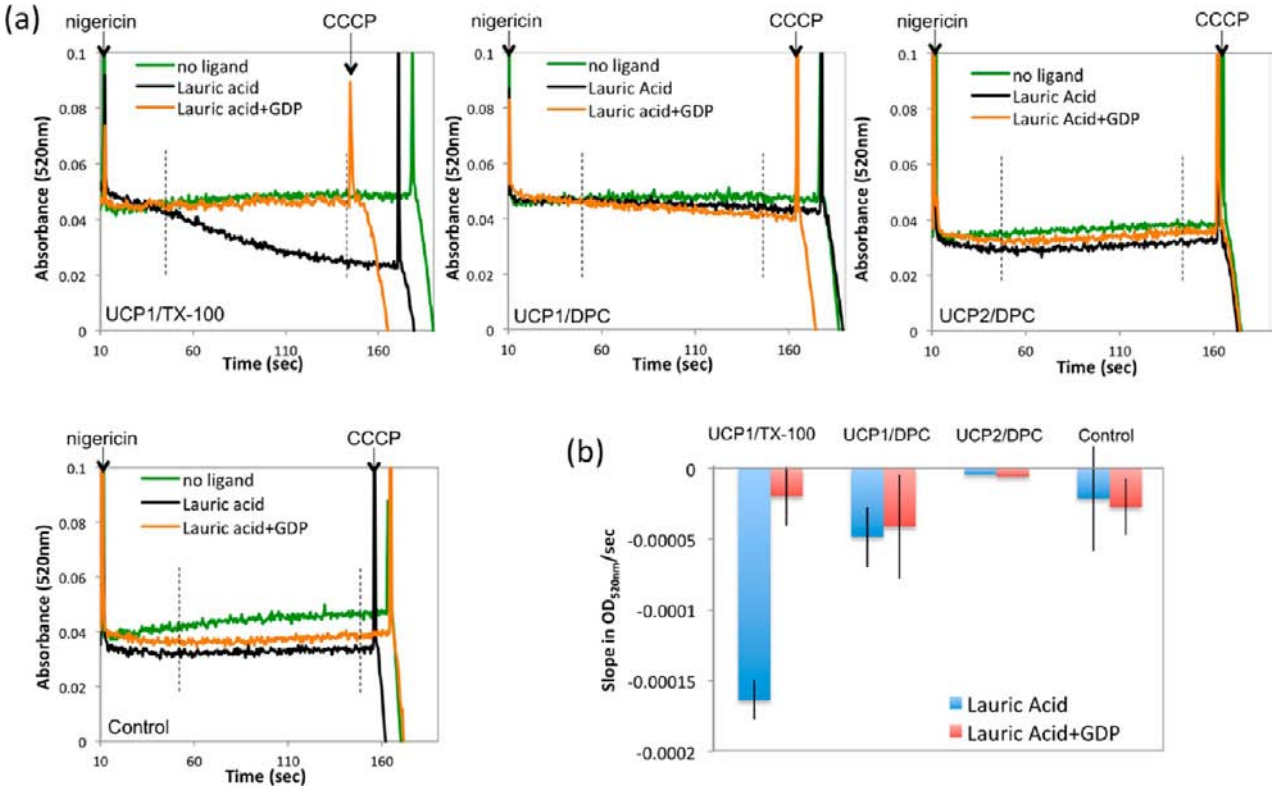

Figure 5. Functional assay of UCP1 and UCP2 after reconstitution in liposomes. (a) Kinetics curves of the safranine O polarization monitored at 520 nm. The arrows indicate the addition of nigericin and CCCP (the addition of ligands being done before nigericin). The delimited time scale for the slope determination is indicated on the graphs by dashed vertical lines. (b) Histogram reflecting the proton transport activity of UCP1 and UCP2. The bars show the differences in polarization slopes of the safranine O after subtraction of the background, i.e., no ligand. Activation of the proton transport was monitored in the presence of lauric acid whereas inhibition was monitored in the presence of both lauric acid and GDP (for details see the Methods section).

residues distributed along helix 2 (residues 76−110) and exposed toward the detergent bundle (see Figure S3).

■ DISCUSSION

Painting a detailed picture of mitochondrial communication relies on high-resolution structural information, the production of which remains a daunting challenge owing to the considerable difficulty to express and purify mitochondrial carriers, and ultimately determine the structure, either by crystallography or by NMR. Associating NMR data with molecular-fragment replacement, Berardi et al.[22] succeeded in obtaining a three-dimensional structure of an uncoupling protein, UCP2, binding an inhibitor, GDP^{3-}, solubilized by DPC (pdb:2LCK). The UCP2 structure surrounded by DPC molecules is stable in our MD simulations, suggesting that their model is relevant in this detergent.

Moreover, their study suggests that the structure of UCP2 closely resembles that of AAC. In its crystallographic structure, AAC is in a conformation open toward the intermembrane space, fully occluded on the matrix side and impervious to water or any other small substrate.[19,21,44] The MD simulations performed here enlighten, however, striking differences in the

dx.doi.org/10.1021/ja407424v | J. Am. Chem. Soc. 2013, 135, 15174−15182

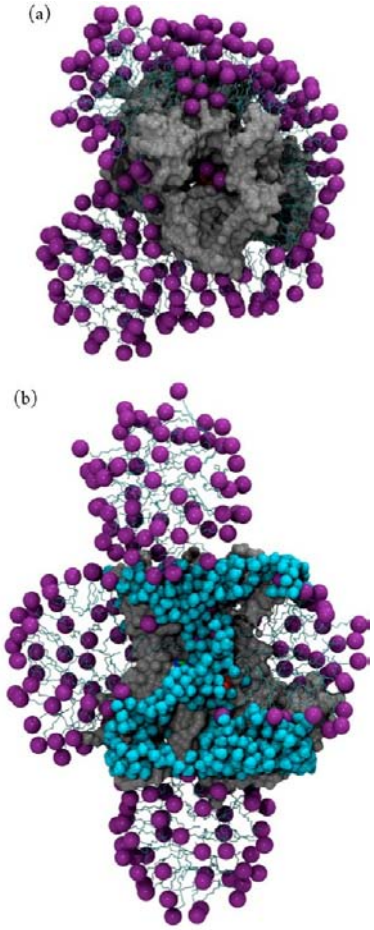

Figure 6. (a). Top view of UCP2-GDP^{3-} embedded in DPC micelles after full relaxation of the entire protein. For clarity, the DPC micelle lying on the cytoplasmic side is not shown. Violet and cyan spheres represent phospholipid headgroups and water molecules, respectively. Phosphorus, nitrogen, oxygen, and carbon of nucleotides are colored in brown, blue, red, and green, respectively. (b) Cross-sectional view of UCP2-GDP^{3-} embedded in DPC micelles after full relaxation of the entire protein. Detergent molecules are organized in a bundle around the hydrophobic core of the protein. Two extra micelles assemble on the matrix and cytoplasmic sides around amphiphilic patches of amino acids. The internal cavity of the protein is fully opened, a conformation akin to that observed in the backbone-constrained simulation

structure of the two proteins. Specifically, our results show that UCP2, wherein the backbone atoms are holonomically constrained, primarily consists of a large water channel connecting the two sides of a POPC membrane, irrespective of the presence of GDP^{3-}. This structural feature is shared by nonselective porins, but not by membrane transporters, and, hence, does not support an alternate access mechanism, in which the conformation of the transporting protein sequentially opens on each side of the membrane. The effective radius of the internal channel of UCP2, ∼6.1 Å, clearly compares to that of toxins or bacterial outer-membrane porins but is much larger than the one measured for aquaporins, a family of membrane channels that selectively conduct water while preventing proton permeation. The continuous water flow across UCP2 is thus likely to allow for proton leakage, a situation that could hardly preserve the proton gradient across the inner membrane of the mitochondria, an absolute requirement for the survival of the organelle. When performed without positional holonomic constraints, the molecular simulations revealed that the NMR structure of UCP2 is not stable in a lipid bilayer environment. The hydrophobic tails of POPC can barely stabilize the cavities found between transmembrane helices and lined with polar and hydrophobic residues. Consequently, the overall tertiary structure rapidly collapses toward a compact arrangement, which remains permeable to water. In contrast, MD simulations of the self-assembly of DPC around UCP2 demonstrate that small detergents can lodge themselves in these cavities and, hence, stabilize the overall NMR protein fold. The thermodynamic parameters of the interaction between two transmembrane helical spans can be affected by DPC as previously reported,[45] indicating that DPC does not behaves as an ideal membrane mimetic environment for some membrane proteins. It is noteworthy that, in spite of what appears to be a partial denaturation of UCP2 in detergent, the network of interactions formed by the protein and its inhibitor is preserved (see Figure S6). This observation is consistent with experimental data based on FRET experiments[22] and atomic force microscopy[46] suggesting that the binding site of UCP2 purified in DPC is preserved. However, retaining GDP^{3-} binding is not sufficient to prove that the protein is fully functional. While it is clearly demonstrated that the protein binds GDP^{3-}, it is difficult to draw definitive conclusions about its proton transport activity for several reasons. For example, if the concentration of activator ligand is above the usual concentration of fatty-acid required either to observe UCP1 activity[4] or to trigger free fatty-acid-mediated proton leakage on mitochondria,[9,47] an unspecific proton leakage may occur through the vesicle walls as exemplified in our proton transport assay (see Figure S7). Reproducing the purification procedure of the recombinant UCP2 in DPC, our functional assay showed no proton transport activity by UCP2. Several studies, performed on the better-characterized native UCP1, showed that the protein tolerates a limited variety of detergents, mainly Triton X-100 and some polyoxyethylene glycols, but not octylglucoside.[5] UCP1 purified in Triton X-100 was fully regulated as expected,[6] while purification of the protein in DPC abolished the activity of UCP1 and its regulation.

Our work highlights how critically important the proper choice of detergent is for membrane protein structure determination. Indeed, while detergents are useful for the solubilization of membrane proteins, they can compete with stabilizing intramolecular interactions within the protein, leading to inactivation.[48,49] The severity of the effect strongly depends on the nature of the membrane proteins, leading one to distinguish between "fragile" and "robust" proteins, which are generally α-helical and β-barrel proteins, and also, eukaryotic and prokaryotic proteins, respectively. As a general rule, the robustness of a membrane protein is correlated to the compactness of interaction networks, which generally increases with the living temperature of the organisms. This feature has created a bias in favor of structural determination of robust membrane proteins. Furthermore, designing a general rule for choosing the detergent suitable for fragile membrane proteins is difficult. Two molecular mechanisms of inactivation of membrane proteins by detergents can be considered. One is the presence of micelles acting as a hydrophobic sink into which stabilizing interacting partners such as lipids, cofactors or protein subunits can disperse, thereby leading to the loss of the protein integrity. Working close to the critical micellar concentration of the detergent can limit this effect. The second mechanism of destabilization, which is the most likely to occur

dx.doi.org/10.1021/ja407424v | J. Am. Chem. Soc. 2013, 135, 15174−15182

in the case of UCPs, is the intrusion of the hydrophobic tails of the detergents between the transmembrane helices. This mechanism can be restrained using a more rigid detergent. For example, novel DDM analogues with multiple, branched, or cyclic hydrophobic moieties presenting less flexibility than DDM have been shown to improve the stability of several membrane proteins.[50−52] Many other alternatives to replace detergents have been developed, among which are fluorinated detergents, nanodiscs, and amphipols (for review see Popot[53]). All these innovative surfactants improve the stability of membrane proteins, but require a previous solubilization step with conventional detergents. Finally, it should be stressed that genetic engineering of membrane proteins has been highly successful in improving the thermostability of G protein-coupled receptors.[54] This strategy might also benefit other classes of membrane proteins, including the mitochondrial carriers.

■ CONCLUSION

While acquiring precise structural information is crucial for a full understanding of the biological processes like transport mechanisms of mitochondrial carriers, assessing the physiological relevance of the newly solved three-dimensional structures is equally crucial. A recent study revealed indeed that detergents can cause structural perturbations and distortions leading to unsuitable interpretations as to the molecular mechanisms of some membrane proteins.[27] As exemplified in this study, a combination of theoretical and functional investigations represents an appealing and promising strategy, the frontiers of which go beyond the family of mitochondrial transporters to embrace most membrane proteins. This work further emphasizes that molecular simulations not only can be employed to rationalize and predict the properties of membrane proteins near their equilibrium conformation, but can also address the physiological relevance of structures obtained in non-native environments. Our data strongly suggest that the structure of UCP2 in DPC is not physiologically relevant and, therefore, that it may be misleading to use it as a basis for drawing inferences about the physiological behavior of members of the MCF. For membrane proteins like UCP2—which expose not only nonpolar contacts to the hydrophobic core of the membrane, but also a number of weakly polar contacts—it is preferable to avoid small, flexible detergents, which can easily target these two types of interactions simultaneously.

■ METHODS

Purification of UCP1 and UCP2. BAT was kindly provided by V. Lenoir (ICGM), Paris, France from mice cold-adapted for 2 days. The purification of UCP1 was carried out as described by Lin and Klingenberg.[38] Mitochondria were isolated from BAT and washed out with 3.2% Lubrol WX in buffer 20 mM MOPS, 20 mM Na_2SO_4, 0.16 mM EDTA, pH 6.9. The mitochondrial membranes were split in two. The total mitochondrial proteins were solubilized using either Triton X-100 with a w/w protein:detergent ratio of 1:1.6 or DPC with a ratio 1:1. The extracts were centrifuged and then applied to a hydroxyapatite column (BioRad). The flow-through fractions containing UCP1 were collected, and the purity was controlled by SDS-PAGE with 12% acrylamide gels (Invitrogen). The production of UCP2 was adapted from Berardi et al.[22] The cDNA of mouse UCP2 encoding for residues 14−309 was cloned into a pET-22b vector between the restriction sites *Nde*I and *Eco*RI. The protein was overexpressed in *E. coli* Rosetta λ(DE3). The concentration of total proteins present in the 50000*g* pellet was determined by a BCA assay. UCP2 was solubilized in DPC with a w/w protein:detergent ratio of 1:3 in buffer 20 mM Tris, 150 mM NaCl, pH 8. After 30 min of incubation at 4 °C, the sample was centrifuged at 100000*g* for 20 min. The supernatant was then loaded onto a Ni-NTA column (Thermo Scientific) and elution occurred with 300 mM imidazole. The fraction containing UCP2 was dialyzed and then applied to an ion exchange column (GE Healthcare) for further purification. The purity of the flow-through fractions was controlled by SDS-PAGE. The band corresponding to UCP2 on the gel was cut off for further analysis by MALDI-TOF mass spectrometry, confirming the expected UCP2 protein.

Functional Assay. The functional assay was carried out as described in Mozo et al.[6] Small unilamellar vesicles composed by phosphatidylcholine, phosphatidylethanolamine, and cardiolipin in a w/w/w ratio of 80:80:10 were prepared by sonication in buffer 20 mM KH_2PO_4, 70 mM K_2SO_4, pH 6.9, at a final concentration of 10 mg/mL. The proteoliposomes were prepared by mixing UCP samples, vesicles, and buffer in a v/v/v ratio of 1:8:4 and incubated for 1 h at room temperature under shaking. For UCP purified in DPC, the protein incorporation in liposomes was facilitated by supplying Triton X-100 (2%) to the sample. The detergent was removed by adsorption onto biobeads (BioRad), and the liposomes where then dialyzed three times for 1 h against a buffer containing 200 mM sucrose, 0.5 mM Hepes, and 0.5 mM EDTA, pH 6.8. For each measure, an aliquot of the liposomes suspension (100 μL) was mixed with 2 mL of 100 mM choline choride, 20 μM safranine O. The absorption of safranine O was recorded at 520 nm with a UV−visible spectrophotometer. All ligands are added first in order to avoid any perturbation of the absorbance baseline. The activation experiments were recorded by supplying lauric acid (30 μM) in the cuvette, while for inhibition experiments both lauric acid (30 μM) and GDP^{3-} (50 μM) were added. The proton transport was activated upon addition of nigericin (0.1 μM), which generates the pH gradient. At the end of the kinetics, CCCP (5 μM) was added to measure the complete polarization of liposomes, giving an indication of the internal volume of the liposomes. The slopes of the curves were determined between 50 and 150 s, and the background of the basal activity (in the absence of ligand) was subtracted in order to observe the ligand effects only. The activity measurements for UCP1 were repeated from three independent purifications and then averaged.

All-Atom Molecular Dynamics. Three different molecular assays were built based on the UCP2 NMR structure. A first setup was obtained by inserting the protein into a fully hydrated bilayer of 146 POPC lipids, using the membrane builder module of CHARMM-GUI (http://www.charmm-gui.org/).[55] Docking of a GDP^{3-} anion inside UCP2 internal cavity, at a position consistent with the NMR prediction, provided a second initial configuration. Finally, we performed several all-atom and coarse-grained MD simulations (see Supplementary Methods) to study self-aggregation of DPC at 200 μM around the protein at various detergent:protein ratios. We superimposed the final configuration of all trajectories and built an all-atom model, including GDP^{3-}, and integrating all observed DPC−protein interactions, for a total of 300 DPC molecules. Respectively 14 and 17 chloride anions were added to setups with and without GDP^{3-} to ensure electric neutrality. MD simulations were carried out with the NAMD[56] program. Setups and analyses were performed using VMD.[57] All trajectories were generated in the isobaric−isothermal ensemble, at 300 K under 1 atm using, respectively, Langevin dynamics[58] (damping coefficient, 1 ps^{-1}) and the Langevin piston[59] method. The particle mesh Ewald (PME) algorithm[60] was used to account for long-range electrostatic interactions. Covalent bonds involving hydrogen atoms were constrained to their equilibrium length by means of the Rattle algorithm.[53] The equations of motion were integrated by means of a multiple-time step algorithm[62] with a time step of 2 and 4 fs for short- and long-range interactions, respectively. The CHARMM force field[63−65] including CMAP[66] corrections was employed to model proteins, POPC lipids or DPC detergents, GDP^{3-}, and counterions; the TIP3P[67] model was used to describe water. Water, lipids or detergents, substrate, and counterions were first thermalized for 20 ns, while the entire protein was kept fixed. For the next 20 ns, the constraints on the side chains were removed, and only the backbone

was constrained to its NMR conformation. For UCP2 associated to GDP^{3-}, simulations in POPC and DPC were extended further up to 175 ns without any positional constraints.

Permeability Methods. To calculate the osmotic permeability of the UCP2 structures, we followed the algorithm described by Aksimentiev and Schulten.[35] The pore of the structure given by NMR had a more complex topology and structure than the α-hemolysin channel; we, therefore, calculated the permeability only over the central region of the pore where the topology was simpler and relatively stable among the simulations. The region was delineated by two approximately coplanar rings of Cα atoms, with one atom chosen from each of the six transmembrane helices. Let R_0 and R_1 be the centers of mass of the bottom and top rings, respectively, consisting of the Cα atoms of residues 34, 85, 137, 181, 239, and 274, and residues 20, 101, 120, 194, 227, and 288. The region considered had the form of a cylinder with a base at R_0 and axis lying along the vector $R_1 - R_0$. The length of the cylinder along the axis was L = 19.5 Å, equivalent to the distance $|R_1 - R_0|$ for the NMR structure. The radius of the cylinder was chosen to be 20 Å, which was large enough to encompass all water molecules between the two rings. The collective displacement of the water molecules within the protein at time $t + \Delta t$ of the simulation trajectory was calculated as

$$n(t + \Delta t) = n(t) + \sum_{i \in S(t,t+\Delta t)} \frac{\Delta r_i \cdot e}{L}$$

where $S(t,t+\Delta t)$ is the union of subsets of water molecules within the cylinder at time t and $t+\Delta t$, Δr_i is the displacement of water molecule i between time t and $t+\Delta t$, and e is the unit vector along $R_1 - R_0$. The displacements of water molecules entering or leaving the region between the frames were truncated at the boundary of the region. The calculation was performed with Δt = 10 ps. The collective diffusion coefficient, D_n, was obtained from $\langle n(t) \rangle^2 = 2D_n t$, where the average was performed over 100 subtrajectories each 10 ps in length. The permeability was calculated as $P_f = v_w D_n$, where v_w was the average volume of a water molecule. Further, following Aksimentiev and Schulten, the resulting permeabilities were scaled by 1/2.87 to account for the difference in the viscosity of the TIP3P water model and real water.[35]

■ ASSOCIATED CONTENT

Supporting Information

Methodological details and supplementary experimental and theoretical data. This material is available free of charge via the Internet at http://pubs.acs.org.

■ AUTHOR INFORMATION

Corresponding Authors

bruno.miroux@ibpc.fr
francois.dehez@univ-lorraine.fr

Notes

The authors declare no competing financial interest.

■ ACKNOWLEDGMENTS

We thank O. Ilioaia for helping in bacterial membrane preparation and V. Lenoir for providing BAT from cold-adapted mice. D. Warchawski, L. Catoire, K. Moncoq, and D. Picot are acknowledged for helpful discussions. We thank J.-L. Popot for insightful comments on the manuscript. This work was supported by the Agence National de La Recherche (ANR MIT-2M, No. ANR 2010 BLAN1518), the "Initiative d'excellence" program from the French State (DYNAMO, ANR-11-LABX-0011-01), and the Direction Régionale à la Recherche et à la Technologie de Lorraine. The Grand Equipement National de Calcul Informatique (GENCI) and the Centre Informatique National de l'Enseignement Supérieur (CINES) are gratefully acknowledged for the provision of computer time.

■ REFERENCES

(1) Rousset, S.; Alves-Guerra, M.-C.; Mozo, J.; Miroux, B.; Cassard-Doulcier, A.-M.; Bouillaud, F.; Ricquier, D. *Diabetes* **2004**, *53*, 130S−135.
(2) Kunji, E. R. S. *FEBS Lett.* **2004**, *564*, 239−244.
(3) Enerbäck, S.; Jacobsson, A.; Simpson, E. M.; Guerra, C.; Yamashita, H.; Harper, M.-E.; Kozak, L. P. *Nature* **1997**, *387*, 90−94.
(4) Winkler, E.; Klingenberg, M. *J. Biol. Chem.* **1994**, *269*, 2508−2515.
(5) Winkler, E.; Klingenberg, M. *Eur. J. Biochem.* **1992**, *207*, 135−145.
(6) Mozo, J.; Ferry, G.; Masscheleyn, S.; Miroux, B.; Boutin, J. A.; Bouillaud, F. *Anal. Biochem.* **2006**, *351*, 201−206.
(7) Blesneac, I.; Ravaud, S.; Machillot, P.; Zoonens, M.; Masscheylen, S.; Miroux, B.; Vivaudou, M.; Pebay-Peyroula, E. *Eur. Biophys. J.* **2012**, *41*, 675−679.
(8) Rial, E.; Poustie, A.; Nicholls, D. G. *Eur. J. Biochem.* **1983**, *137*, 197−203.
(9) Rial, E.; Aguirregoitia, E.; Jiménez-Jiménez, J.; Ledesma, A. *Biochim. Biophys. Acta BBA—Bioenerg.* **2004**, *1608*, 122−130.
(10) Mozo, J.; Ferry, G.; Studeny, A.; Pecqueur, C.; Rodriguez, M.; Boutin, J. A.; Bouillaud, F. *Biochem. J.* **2006**, *393*, 431−439.
(11) Pecqueur, C.; Bui, T.; Gelly, C.; Hauchard, J.; Barbot, C.; Bouillaud, F.; Ricquier, D.; Miroux, B.; Thompson, C. B. *FASEB J. Off. Publ. Fed. Am. Soc. Exp. Biol.* **2008**, *22*, 9−18.
(12) Fedorenko, A.; Lishko, P. V.; Kirichok, Y. *Cell* **2012**, *151*, 400−413.
(13) Echtay, K. S.; Winkler, E.; Frischmuth, K.; Klingenberg, M. *Proc. Natl. Acad. Sci. U.S.A.* **2001**, *98*, 1416−1421.
(14) González-Barroso, M. M.; Fleury, C.; Bouillaud, F.; Nicholls, D. G.; Rial, E. *J. Biol. Chem.* **1998**, *273*, 15528−15532.
(15) Emre, Y.; Hurtaud, C.; Karaca, M.; Nubel, T.; Zavala, F.; Ricquier, D. *Proc. Natl. Acad. Sci. U.S.A.* **2007**, *104*, 19085−19090.
(16) Mattiasson, G.; Shamloo, M.; Gido, G.; Mathi, K.; Tomasevic, G.; Yi, S.; Warden, C. H.; Castilho, R. F.; Melcher, T.; Gonzalez-Zulueta, M.; Nikolich, K.; Wieloch, T. *Nat. Med.* **2003**, *9*, 1062−1068.
(17) Vogler, S.; Pahnke, J.; Rousset, S.; Ricquier, D.; Moch, H.; Miroux, B.; Ibrahim, S. M. *Am. J. Pathol.* **2006**, *168*, 1570−1575.
(18) Bouillaud, F. *BBA-Bioenerg.* **2009**, *1787*, 377−383.
(19) Dehez, F.; Pebay-Peyroula, E.; Chipot, C. *J. Am. Chem. Soc.* **2008**, *130*, 12725−12733.
(20) Kunji, E. R. S.; Harding, M. *J. Biol. Chem.* **2003**, *278*, 36985−36988.
(21) Pebay-Peyroula, E.; Dahout-Gonzalez, C.; Kahn, R.; Trézéguet, V.; Lauquin, G. J.-M.; Brandolin, G. *Nature* **2003**, *426*, 39−44.
(22) Berardi, M. J.; Shih, W. M.; Harrison, S. C.; Chou, J. J. *Nature* **2011**, *476*, 109−113.
(23) Cross, T. A.; Sharma, M.; Yi, M.; Zhou, H.-X. *Trends Biochem. Sci.* **2011**, *36*, 117−125.
(24) Smith, S. O.; Song, D.; Shekar, S.; Groesbeek, M.; Ziliox, M.; Aimoto, S. *Biochemistry (Mosc.)* **2001**, *40*, 6553−6558.
(25) Bond, P. J.; Cuthbertson, J. M.; Deol, S. S.; Sansom, M. S. P. *J. Am. Chem. Soc.* **2004**, *126*, 15948−15949.
(26) Bond, P. J.; Faraldo-Gómez, J. D.; Deol, S. S.; Sansom, M. S. P. *Proc. Natl. Acad. Sci. U.S.A.* **2006**, *103*, 9518−9523.
(27) Zhou, H.-X.; Cross, T. A. *Annu. Rev. Biophys.* **2013**, *42*, 361−392.
(28) Hong, H.; Bowie, J. U. *J. Am. Chem. Soc.* **2011**, *133*, 11389−11398.
(29) Shi, L.; Zheng, H.; Zheng, H.; Borkowski, B. A.; Shi, D.; Gonen, T.; Jiang, Q.-X. *Proc. Natl. Acad. Sci. U.S.A.* **2013**, *110*, 3369−3374.
(30) Lu, G. J.; Tian, Y.; Vora, N.; Marassi, F. M.; Opella, S. J. *J. Am. Chem. Soc.* **2013**, *135*, 9299−9302.
(31) Nury, H.; Dahout-Gonzalez, C.; Trézéguet, V.; Lauquin, G. J. M.; Brandolin, G.; Pebay-Peyroula, E. *Annu. Rev. Biochem.* **2006**, *75*, 713−741.

(32) Wang, Y.; Tajkhorshid, E. *Proc. Natl. Acad. Sci. U.S.A.* **2008**, *105*, 9598−9603.
(33) Mifsud, J.; Ravaud, S.; Krammer, E.-M.; Chipot, C.; Kunji, E. R. S.; Pebay-Peyroula, E.; Dehez, F. *Mol. Membr. Biol.* **2013**, *30*, 160−168.
(34) Pebay-Peyroula, E.; Brandolin, G. *Curr. Opin. Struct. Biol.* **2004**, *14*, 420−425.
(35) Aksimentiev, A.; Schulten, K. *Biophys. J.* **2005**, *88*, 3745−3761.
(36) Robertson, K. M.; Tieleman, D. P. *FEBS Lett.* **2002**, *528*, 53−57.
(37) Zhu, F.; Tajkhorshid, E.; Schulten, K. *Phys. Rev. Lett.* **2004**, *93*, 224501−224504.
(38) Lin, C. S.; Klingenberg, M. *FEBS Lett.* **1980**, *113*, 299−303.
(39) Krämer, R.; Klingenberg, M. *FEBS Lett.* **1977**, *82*, 363−367.
(40) Bond, P. J.; Sansom, M. S. P. *J. Am. Chem. Soc.* **2006**, *128*, 2697−2704.
(41) Timmins, P.; Pebay-Peyroula, E.; Welte, W. *Biophys. Chem.* **1994**, *53*, 27−36.
(42) Pebay-Peyroula, E.; Garavito, R.; Rosenbusch, J.; Zulauf, M.; Timmins, P. *Structure* **1995**, *3*, 1051−1059.
(43) Abel, S.; Dupradeau, F.-Y.; Marchi, M. *J. Chem. Theory Comput.* **2012**, *8*, 4610−4623.
(44) Krammer, E.-M.; Ravaud, S.; Dehez, F.; Frelet-Barrand, A.; Pebay-Peyroula, E.; Chipot, C. *Biophys. J.* **2009**, *97*, L25−L27.
(45) Mineev, K. S.; Khabibullina, N. F.; Lyukmanova, E. N.; Dolgikh, D. A.; Kirpichnikov, M. P.; Arseniev, A. S. *Biochim. Biophys. Acta BBA—Biomembr.* **2011**, *1808*, 2081−2088.
(46) Zhu, R.; Rupprecht, A.; Ebner, A.; Haselgrübler, T.; Gruber, H. J.; Hinterdorfer, P.; Pohl, E. E. *J. Am. Chem. Soc.* **2013**, *135*, 3640−3646.
(47) Jaburek, M. *J. Biol. Chem.* **2003**, *278*, 25825−25831.
(48) Bowie, J. U. *Curr. Opin. Struct. Biol.* **2001**, *11*, 397−402.
(49) Garavito, R. M.; Ferguson-Miller, S. *J. Biol. Chem.* **2001**, *276*, 32403−32406.
(50) Chae, P. S.; Rasmussen, S. G. F.; Rana, R. R.; Gotfryd, K.; Chandra, R.; Goren, M. A.; Kruse, A. C.; Nurva, S.; Loland, C. J.; Pierre, Y.; Drew, D.; Popot, J.-L.; Picot, D.; Fox, B. G.; Guan, L.; Gether, U.; Byrne, B.; Kobilka, B.; Gellman, S. H. *Nat. Methods* **2010**, *7*, 1003−1008.
(51) Hong, W.-X.; Baker, K. A.; Ma, X.; Stevens, R. C.; Yeager, M.; Zhang, Q. *Langmuir* **2010**, *26*, 8690−8696.
(52) Hovers, J.; Potschies, M.; Polidori, A.; Pucci, B.; Raynal, S.; Bonneté, F.; Serrano-Vega, M. J.; Tate, C. G.; Picot, D.; Pierre, Y.; Popot, J.-L.; Nehmé, R.; Bidet, M.; Mus-Veteau, I.; Bußkamp, H.; Jung, K.-H.; Marx, A.; Timmins, P. A.; Welte, W. *Mol. Membr. Biol.* **2011**, *28*, 171−181.
(53) Popot, J.-L. *Annu. Rev. Biochem.* **2010**, *79*, 737−775.
(54) Tate, C. G.; Schertler, G. F. *Curr. Opin. Struct. Biol.* **2009**, *19*, 386−395.
(55) Jo, S.; Lim, J. B.; Klauda, J. B.; Im, W. *Biophys. J.* **2009**, *97*, 50−58.
(56) Phillips, J. C.; Braun, R.; Wang, W.; Gumbart, J.; Tajkhorshid, E.; Villa, E.; Chipot, C.; Skeel, R. D.; Kalé, L.; Schulten, K. *J. Comput. Chem.* **2005**, *26*, 1781−1802.
(57) Humphrey, W.; Dalke, A.; Schulten, K. *J. Mol. Graph.* **1996**, *14*, 33−38.
(58) Feller, S. E.; Zhang, Y.; Pastor, R. W.; Brooks, B. R. *J. Chem. Phys.* **1995**, *103*, 4613.
(59) Martyna, G. J.; Tobias, D. J.; Klein, M. L. *J. Chem. Phys.* **1994**, *101*, 4177.
(60) Darden, T.; York, D.; Pedersen, L. *J. Chem. Phys.* **1993**, *98*, 10089.
(61) Andersen, H. C. *J. Comput. Phys.* **1983**, *52*, 24−34.
(62) Tuckerman, M.; Berne, B. J.; Martyna, G. J. *J. Chem. Phys.* **1992**, *97*, 1990.
(63) MacKerell, A. D., Jr.; Bashford, D.; Bellott, M.; Dunbrack, R. L., Jr.; Evanseck, J. D.; Field, M. J.; Fischer, S.; Gao, J.; Guo, H.; Ha, S.; Joseph-McCarthy, D.; Kuchnir, L.; Kuczera, K.; Lau, F. T. K.; Mattos, C.; Michnick, S.; Ngo, T.; Nguyen, D. T.; Prodhom, B.; Reiher, W. E.; Roux, B.; Schlenkrich, M.; Smith, J. C.; Stote, R.; Straub, J.; Watanabe, M.; Wiórkiewicz-Kuczera, J.; Yin, D.; Karplus, M. *J. Phys. Chem. B* **1998**, *102*, 3586−3616.
(64) Foloppe, N.; MacKerell, A. D., Jr. *J. Comput. Chem.* **2000**, *21*, 86−104.
(65) Klauda, J. B.; Venable, R. M.; Freites, J. A.; O'Connor, J. W.; Tobias, D. J.; Mondragon-Ramirez, C.; Vorobyov, I.; MacKerell, A. D.; Pastor, R. W. *J. Phys. Chem. B* **2010**, *114*, 7830−7843.
(66) MacKerell, A. D.; Feig, M.; Brooks, C. L. *J. Am. Chem. Soc.* **2004**, *126*, 698−699.
(67) Jorgensen, W. L.; Chandrasekhar, J.; Madura, J. D.; Impey, R. W.; Klein, M. L. *J. Chem. Phys.* **1983**, *79*, 926.